IJARSCT

International Journal of Advanced Research in Science, Communication and Technology

International Open-Access, Double-Blind, Peer-Reviewed, Refereed, Multidisciplinary Online Journal

ISSN: 2581-9429

Volume 6, Issue 8, April 2026

Impact Factor: 8.2

MHD Flow over a Constant Wedge Embedded in a Porous Medium with Secord-Order Slip

Nasreen Bano[1] **and S. R. Sayyed**[2]
[1]G. M. Vedak College of Science, Tala-Raigad
[2]Mangaon Taluka Education Society's
Doshi Vakil Arts College and G.C.U.B. Science & Commerce College, Goregaon-Raigad

Abstract: *This paper deals with a steady two-dimensional magnetohydrodynamic (MHD) boundary-layer slip flow of an incompressible, viscous, and electrically conducting fluid over a stationary wedge situated within a porous medium in presence of second-order slip condition. The external stream velocity follows a power-law distribution, while suction or injection is imposed at the surface. By employing similarity transformations, the governing nonlinear partial differential equations are reduced to a nonlinear ordinary differential equation. An analytical approach is implemented to obtain solutions. The impacts of magnetic parameter, permeability parameter, suction/injection parameter, pressure gradient parameter, and velocity slip parameter are systematically examined. The solutions demonstrate excellent convergence characteristics and strong agreement with available published results.*

Keywords: Magnetohydrodynamics; Porous Medium and Slip Flow

1. Introduction

The investigation of boundary-layer flow over a stationary wedge originates from the classical work of Falkner and Skan [1], who demonstrated how Prandtl's boundary-layer equations can be transformed into a nonlinear ordinary differential equation through an appropriate similarity transformation. Their formulation stimulated extensive research activity, and numerous contributions to this topic can be found in Schlichting and Gersten [2], Leal [3], and Ishak et al. [4].

Magnetohydrodynamic (MHD) boundary-layer flow over wedge geometries has attracted considerable interest due to its broad engineering relevance. Applications include MHD generators, nuclear reactor cooling systems, polymer extrusion processes, electromagnetic propulsion devices, and fluid flow in spinning and manufacturing operations. Andersson [5] examined the behavior of viscous fluid flow past a stretching surface in the presence of magnetic effects. Raptis et al. [6] analyzed the role of thermal radiation in MHD flow problems. The two-dimensional MHD stagnation-point flow of a viscous fluid over a nonlinear stretching surface was investigated by Hayat et al. [7]. Rashidi and Erfani [8] studied similarity solutions for MHD flow adjacent to a flat plate with variable wall temperature embedded in a porous medium. Kudenatti et al. [9] further explored the two-dimensional MHD flow of a viscous fluid over a wedge placed in a porous environment.

Most of the aforementioned investigations were conducted under the assumption of a no-slip boundary condition. However, in practical situations involving micro-scale flows, suspensions, emulsions, polymeric fluids, and nano-fluidic systems, the classical no-slip condition may not accurately describe the physics at the solid boundary. In such cases, velocity slip at the surface becomes significant. The phenomenon of slip flow has been extensively discussed in earlier studies [10]. More recently, several researchers [11, 12, 13] have examined boundary-layer flows incorporating velocity slip effects. Slip boundary conditions have important technological applications, particularly in coating processes and polishing operations within artificial cavities.

To the best of our knowledge, the steady two-dimensional magnetohydrodynamic (MHD) boundary-layer slip flow of an incompressible, viscous, and electrically conducting fluid over a stationary wedge situated within a porous medium in presence of second-order slip condition has not yet been addressed through a purely analytical framework. In the

DOI: 10.48175/IJARSCT-33151

present work, the coupled nonlinear ordinary differential equations governing this configuration are solved using the Mathematica-based package BVPh 2.0 [14], which is specifically designed for nonlinear boundary-value and eigenvalue problems involving coupled ODE systems. The computational framework is built upon the homotopy analysis method (HAM) [15, 16], an established analytical technique for handling strongly nonlinear differential equations.

The BVPh 2.0 package [14] represents a HAM-based computational platform that facilitates the analytical treatment of nonlinear boundary-value and eigenvalue problems described by coupled ordinary differential equations. The software is freely accessible online (http://numericaltank.sjtu.edu.cn/BVPh.htm).

The present study aims to extend a comprehensive analytical study to analyze MHD boundary-layer flow over a constant wedge embedded in a porous medium, incorporating second-order slip condition. Comparisons of the obtained results with those reported by Kudenatti et al. [9] demonstrate excellent agreement. Furthermore, graphical analysis of the velocity distribution indicates that the dimensionless velocity increases with increasing values of the slip parameter Lunder both suction and injection conditions.

2. Mathematical Formulation and Similarity Analysis

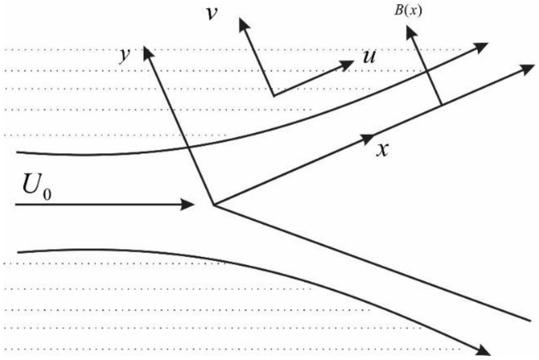

This section presents the mathematical development of the MHD slip flow over a constant wedge embedded in a porous medium. All governing equations, transformations, and the resulting ordinary differential equation are expressed in

$$\nabla \cdot \vec{q} = 0 \tag{1}$$

$$\left(\frac{1}{\varepsilon^2}\right)(\vec{q} \cdot \nabla)\vec{q} = -\left(\frac{1}{\rho}\right)\nabla p + \left(\frac{\mu e}{\rho}\right)\nabla^2\vec{q} - \left(\frac{\mu}{\rho K}\right)\vec{q} + \left(\frac{1}{\rho}\right)(\vec{J} \times \vec{B}) \tag{2}$$

$$\vec{J} = \sigma(\vec{E} + \vec{q} \times \vec{B}) \tag{3}$$

$$\vec{J} \times \vec{B} = -\sigma B^2 \vec{q} \tag{4}$$

Applying boundary-layer approximations, the reduced equations become:

$$\frac{\partial u}{\partial x} + \frac{\partial v}{\partial y} = 0 \tag{5}$$

$$\left(\frac{1}{\varepsilon^2}\right)\left(u\frac{\partial u}{\partial x} + v\frac{\partial u}{\partial y}\right) = -\left(\frac{1}{\rho}\right)\frac{\partial p}{\partial x} + \nu\frac{\partial^2 u}{\partial y^2} - \left(\frac{\nu}{K}\right)u - \left(\frac{\sigma B^2}{\rho\varepsilon}\right)u \tag{6}$$

$$\frac{\partial p}{\partial y} = 0 \tag{7}$$

At the edge of the boundary layer, matching with inviscid flow yields:

$$\left(\frac{U(x)}{\varepsilon^2}\right)\frac{dU(x)}{dx} = -\left(\frac{1}{\rho}\right)\frac{dp}{dx} - \left(\frac{\nu}{K}\right)U(x) - \left(\frac{\sigma B^2}{\rho\varepsilon}\right)U(x) \tag{8}$$

The boundary-layer equation is therefore written as:

DOI: 10.48175/IJARSCT-33151

IJARSCT
International Journal of Advanced Research in Science, Communication and Technology
International Open-Access, Double-Blind, Peer-Reviewed, Refereed, Multidisciplinary Online Journal
ISSN: 2581-9429
Volume 6, Issue 8, April 2026
Impact Factor: 8.2

$$\left(\frac{1}{\varepsilon^2}\right)\left(u\frac{\partial u}{\partial x}+v\frac{\partial u}{\partial y}\right)=\left(\frac{U(x)}{\varepsilon^2}\right)\frac{dU(x)}{dx}+\nu\frac{\partial^2 u}{\partial y^2}-\left(\frac{\nu}{K}\right)\left(u-U(x)\right)-\left(\frac{\sigma B^2}{\rho}\right)\left(u-U(x)\right) \tag{9}$$

Boundary conditions:

$$u\ =A\frac{\partial u}{\partial y}+B\frac{\partial^2 u}{\partial y^2}\ \ v=V_w\ \ at\ y=0 \tag{10}$$

$$u\ \rightarrow\ U(x)\ as\ \ y\ \rightarrow\ \infty \tag{11}$$

Similarity transformations are introduced as:

$$\psi\ =\sqrt{\frac{2\nu xU(x)\varepsilon^2}{1+m}}f(\eta) \tag{12}$$

$$\eta\ =\sqrt{\frac{(1+m)U(x)}{2\varepsilon^2\nu x}}y \tag{13}$$

Using these transformations, the final nonlinear ODE becomes:

$$f'''+f\,f''+\beta(1-(f')^2)+(\Omega+M^2)(1-f')=0 \tag{14}$$

Boundary conditions in similarity form:

$$f(0)=f_w$$

$$f'(0)=L_1\,f''(0)+L_2f'''(0) \tag{15}$$

$$f'(\infty)=1$$

Here, the prime symbol denotes differentiation with respect to the similarity variable η. The function $f(\eta)$ represents the dimensionless stream function. The suction/injection parameter is defined as:

$$f_w\ =-\left(\frac{1}{\varepsilon}\right)\sqrt{\frac{2x}{(m+1)\nu U(x)}}V_w \tag{16}$$

where $f_w > 0$ corresponds to suction and $f_w < 0$ corresponds to injection.
The nonlinear pressure gradient parameter is given by:

$$\beta\ =\frac{2m}{m+1} \tag{17}$$

Here $\beta > 0$ represents a favorable pressure gradient and $\beta < 0$ an adverse pressure gradient.
The magnetic (Hartmann) parameter is defined as:

$$M\ =B_0^2\sqrt{\frac{2\sigma\varepsilon}{\rho U_0(m+1)}} \tag{18}$$

The permeability parameter is expressed as:

$$\Omega\ =2\varepsilon^2\left(\frac{U(x)}{\nu}\right)^{m-2}/(K(m+1)Re_x^{m-1} \tag{19}$$

The local Reynolds number is:

$$Re_x=\frac{Ux}{\nu} \tag{20}$$

The first order dimensionless velocity slip parameter is defined as:

$$L_1=\frac{N}{\varepsilon}\sqrt{\frac{(1+m)U(x)\nu}{2x}} \tag{21}$$

DOI: 10.48175/IJARSCT-33151

The second-order dimensionless slip parameter is L_2

3. Analytical Solution via the Homotopy Analysis Method (HAM)

The Homotopy Analysis Method (HAM) provides a powerful semi-analytical framework for solving nonlinear boundary-value and eigenvalue problems. In 2012, Liao introduced the computational package BVPh 2.0, designed for treating coupled nonlinear ordinary differential equations arising in boundary-layer theory. The present nonlinear system governing the flow problem can be systematically handled within this framework. Only the essential steps relevant to the current formulation are outlined below.

Within BVPh 2.0, it is first necessary to define appropriate auxiliary linear operators corresponding to each governing equation, together with the associated boundary conditions. The software allows the use of high-order deformation equations and provides flexibility in selecting convergence-control parameters to ensure series convergence. These parameters are typically determined through minimization of the residual errors of the governing equations.

Following the standard HAM procedure, the solutions for the dimensionless velocity function $f(\eta)$ and temperature (or auxiliary) function $\theta(\eta)$ are expressed in the form of infinite series expansions:

$$f(\eta) = f_0(\eta) + \sum_{m=1}^{\infty} f_m(\eta) \quad (22)$$

$$\theta(\eta) = \theta_0(\eta) + \sum_{m=1}^{\infty} \theta_m(\eta) \quad (23)$$

The higher-order components $f_m(\eta)$ and $\theta_m(\eta)$ are obtained from the m-th order deformation equations. In accordance with the boundary conditions at infinity, the solution structure is chosen as:

$$f(\eta) = \sum_{m=0}^{\infty}\sum_{k=1}^{\infty} a_{m,k}\,\eta^k e^{m\eta} \quad (24)$$

$$\theta(\eta) = \sum_{m=0}^{\infty}\sum_{k=1}^{\infty} b_{m,k}\,\eta^k e^{m\eta}, \quad (25)$$

Here $a_{m,k}$ and $b_{m,k}$ denote unknown coefficients computed iteratively. These expressions guide the selection of suitable auxiliary linear operators.

We select the following linear operators:

$$\mathcal{L}_1(f) = \frac{d^3 f}{d\eta^3} + \frac{d^2 f}{d\eta^2} \quad (26)$$

$$\mathcal{L}_2(\theta) = \frac{d^2\theta}{d\eta^2} - \theta \quad (27)$$

These operators satisfy the properties:

$$\mathcal{L}_1(c_1 + c_2\eta + c_3 e^{-\eta}) = 0 \quad (28)$$

$$\mathcal{L}_2(c_4 e^{\eta} + c_5 e^{-\eta}) = 0 \quad (29)$$

where c_1, c_2, c_3, c_4, and c_5 are arbitrary constants. To initiate the deformation process, the following initial approximations are selected in agreement with the boundary conditions:

$$f_0(\eta) = (1 - \alpha_1)(e^{-\eta} - 1) + \eta + s \quad (30)$$

$$\theta_0(\eta) = e^{-\eta} \quad (31)$$

The auxiliary functions are chosen as:

$$H_f(\eta) = e^{-\eta} \quad (32)$$

$$H_\theta(\eta) = e^{-\eta} \quad (33)$$

With these definitions of auxiliary operators, initial guesses, and auxiliary functions, the BVPh 2.0 package systematically constructs the convergent analytical series solution of the coupled nonlinear system.

4. Results and Discussion

Using the HAM approach, the analytical solutions of the transformed governing equation (14), subject to the boundary conditions (15), have been successfully obtained. To assess the reliability of the present method, the computed results were compared with those reported by Kudenatti et al. [9] for the case $L = 0$ (see Table 1). The comparison demonstrates strong consistency, particularly for the skin-friction coefficient $f''(0)$, confirming the accuracy of the adopted procedure.

Table 1: Comparison of the values of $f''(0)$ with Kudenatti et al. [9] for $L_1 = L_2 = 0$. $M = 1$

f_w	β	$\Omega = 0.1$		$\Omega = 0.5$		$\Omega = 1.0$	
		Exact [9]	Present	Exact [9]	Present	Exact [9]	Present
-2.5	0.5	0.55426	0.55447	0.66494	0.66485	0.79464	0.79473
-1.5	0.5	0.77682	0.77672	0.9221	0.92111	1.05306	0.05312
1.5	0.5	2.38869	2.38856	2.50242	2.50234	2.83615	2.83624
2.5	0.5	3.18651	3.18655	3.28547	3.28533	3.50062	3.50073

To understand the physical behaviour of the flow, the influence of key governing parameters—namely the suction/injection parameter f_w, pressure gradient parameter β, first-order slip parameter L_1 and second-order slip parameter L_2—on the velocity profile f' has been analyzed and illustrated in Figs. 2–5.

Figure 2 illustrates the impact of injection on the velocity distribution, with remaining parameters fixed. In both situations, strengthening the suction/injection parameter f_w increases the velocity magnitude throughout the boundary layer.

Figure 3 demonstrates the effect of the pressure gradient parameter β on the velocity field. The larger values of β result in higher velocity magnitudes and a thinner momentum boundary layer.

The Figure 4 shows the variation of the velocity profile for different values of the first-order velocity slip parameter L_1. The results indicate that increasing L_1 enhances the velocity near the wall and simultaneously reduces the boundary-layer thickness in both physical situations.

Finally, Figure 5 indicates the effect of second-order velocity slip parameter on flow. As the second-order velocity slip parameter increase velocity profiles decreases.

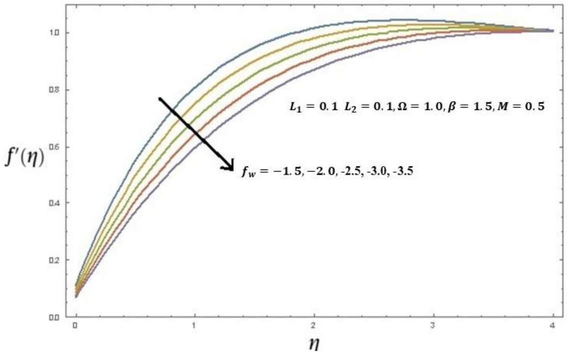

Figure 2: Effect of f_w on $f'(\eta)$

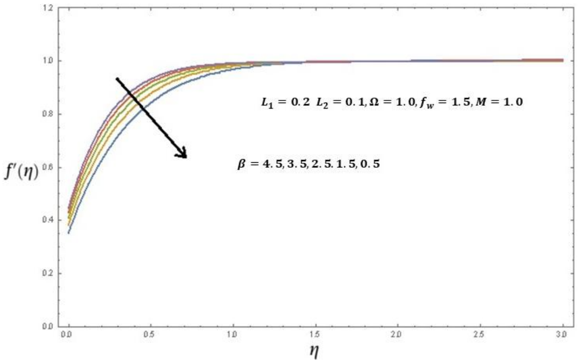

Figure 3: Effect of β on $f'(\eta)$

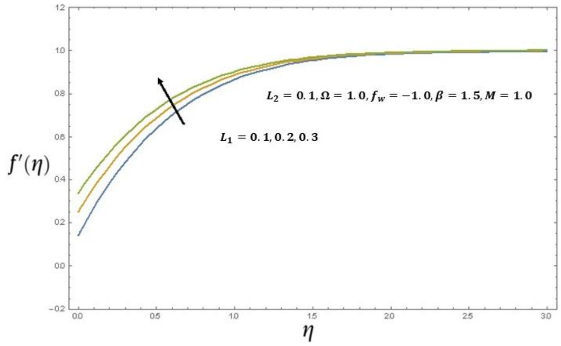

Figure 4: Effect of L_1 on $f'(\eta)$

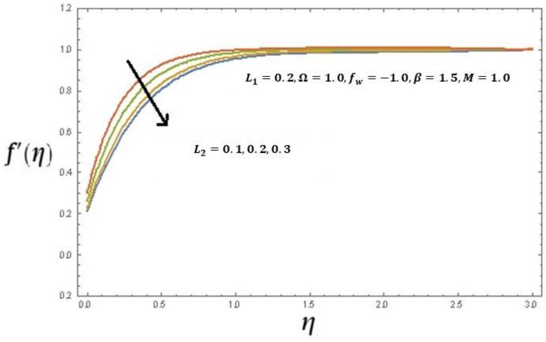

Figure 4: Effect of L_2 on $f'(\eta)$

5. Conclusion

The present study employed the BVPh 2.0 package to derive approximate analytical solutions for magnetohydrodynamic boundary-layer flow over a constant wedge while incorporating velocity slip effects. The obtained results were validated through comparison with the findings of Kudenatti et al. [9], revealing satisfactory agreement and confirming the robustness of the method.

The graphical analysis closely reproduces the trends reported in earlier studies [9]. Furthermore, the investigation demonstrates that an increase in the first-order slip parameter leads to a corresponding increase in velocity and a reduction in boundary-layer thickness.

REFERENCES

[1]. V.M. Falkner, S.W. Skan, Some approximate solutions of the boundary layer equations, Phil. Mag. 12 (1931) 865–896, doi:10.1080/14786443109461870.

[2]. H. Schlichting, K. Gersten, in: Boundary Layer Theory, eighth revised ed., Springer-Verlag, Berlin, 2000.

[3]. L.G. Leal, Advanced Transport Phenomena: Fluid Mechanics and Convective Transport Processes, Cambridge University Press, New York, 2007.

A. Ishak, R. Nazar, I. Pop, Falkner–Skan equation for flow past a moving wedge with suction or injection, J. Appl. Math. Comput. 25 (2007) 67–83, doi:10.1007/bf02832339.

[4]. H.I. Andersson, MHD flow of a viscoelastic fluid past a stretching surface, Acta Mech. 95 (1992) 227–230, doi:10.1007/bf01170814.

A. Raptis, C. Perdikis, H.S. Takhar, Effect of thermal radiation on MHD flow, Appl. Math. Comput. 153 (2004) 645–649, doi:10.1016/s0096-3003(03)00657-x.

[5]. T. Hayat, T. Javed, Z. Abbas, MHD flow of a micropolar fluid near a stagnation-point towards a nonlinear stretching surface, Nonlinear Anal. Real World Appl. 10 (2009) 1514–1526, doi:10.1016/j.nonrwa.2008.01.019.

[6]. M.M. Rashidi, E. Erfani, A new analytical study of MHD stagnation-point flow in porous media with heat transfer, Comput. Fluids 40 (2011) 172–178, doi:10.1016/j.compfluid.2010.08.021.

[7]. R.B. Kudenatti, S.R. Kirsur, A.L. Nargund, N.M. Bujurke, Similarity solutions of the MHD boundary layer flow past a constant wedge within porous media, Math. Probl. Eng. 2017 (2017) 1–11, doi:10.1155/2017/1428137.

A. Yoshimura, R.K. Prud'homme, Wall slip corrections for Couette and parallel disc viscometer, J. Rheol. 32 (1998) 53–67, doi:10.1122/1.549963.

[8]. H.I. Andersson, Slip flow past a stretching surface, Acta Mech. 158 (2002) 121–125, doi:10.1007/bf01463174.

[9]. P.D. Ariel, T. Hayat, S. Asghar, The flow of an elastico-viscous fluid past a stretching sheet with partial slip, Acta Mech. 187 (2006) 29–35, doi:10.1007/s00707-006-0370-3.
[10]. Z. Abbas, Y. Wang, T. Hayat, M. Oberlack, Slip effects and heat transfer analysis in a viscous fluid over an oscillatory stretching sheet, Int. J. Numer. Methods Fluids 59 (2009) 443–458, doi:10.1002/fld.1825.
[11]. Y. Zhao, S. Liao, HAM-based package BVPh 2.0 for nonlinear boundary value problems, in: S. Liao (Ed.),
[12]. Advances in Homotopy Analysis Method, World Scientific Press (2013). doi:10.1142/97898145512500009.
[13]. S.J. Liao, Beyond Perturbation: An Introduction to Homotopy Analysis Method, Chapman & Hall, Boca Raton, FL, 2003, doi:10.1201/9780203491164

DOI: 10.48175/IJARSCT-33151